ELSEVIER

Journal of Nuclear Materials 266–269 (1999) 1097–1102

journal of nuclear materials

Radiative plasma by impurity seeding in W-shaped pumped divertor experiment of JT-60U

K. Itami *, N. Hosogane, S. Konoshima, S. Sakurai, N. Asakura, S. Higashijima, A. Sakasai, H. Tamai, M. Shimada

Japan Atomic Energy Research Institute, Naka Fusion Research Establishment, Naka-machi, Naka-gun, Ibaraki-ken 311-0193, Japan

Abstract

Modification of the divertor to a W-shaped pumped divertor and installation of pumping has enabled demonstration of the 'puff and pump' effect in injected neon, albeit the pumping speed was modest ($\sim$14 m^3/s). It was demonstrated in ELMy H-mode plasmas with $P_{NB} \leqslant 25$ MW that neon seeding and pumping was useful to control the radiation profiles in the main and divertor plasmas, while the large radiation loss from the divertor MARFE was sustained. It was suggested that the neon enrichment in the divertor plasma, which was enhanced by the main D_2 puff, effectively improved the pumping efficiency of neon.

Keywords: JT-60; Radiative divertor; MARFE; Pumped divertor

1. Introduction

Impurity gas injection facilitates radiation profile control in the divertor and main plasma by choosing the amount and atomic numbers of the impurity gas. In the reactor grade devices such as ITER, it is expected that carbon composite targets will be used and that a large portion of power will be dissipated by carbon radiation in the SOL and divertor plasma. Therefore a technique for radiation profile control in the presence of both seeded impurities and carbon must be established in existing large tokamak devices, such as JT-60U.

It was in ELMy H-mode discharges of JT-60U [1,2] that D_2 injection following neon injection effectively promoted dense and cold divertor plasma and triggered the divertor detachment and divertor MARFE. We refer to 'divertor detachment' as the plasma detachment at both the inner and outer divertor striking points in this paper. Since radiation loss peaks near the X-point [3], a divertor MARFE is often called as an X-point MARFE. Radiation loss increased to 70–80% of the input power when a divertor MARFE was established. However it was difficult to control the neon content in the main plasma, since neon was recycling between the main plasma and the first wall. In May 1997, modification of the divertor to a W-shape and the installation of divertor pump [4] were completed to address the advanced control of divertor plasmas. Dynamic control of the radiation profile by controlling neon content is now possible. This paper describes the radiative divertor experiment by neon seeding for the purpose of controlling radiation profiles in the main and divertor plasmas in the W-shaped pumped divertor of JT-60U.

2. Divertor modification and experimental set up

The semi-closed structure of the W-shaped divertor is expected to have better neutral confinement in the divertor region and to facilitate high recycling in the divertor. Neutral particles, escaping through the pumping slot at the bottom of the inner divertor, are then guided under the dome and the outer baffle toward one of the three cryopump systems. These cryopumps used to be a part of the NBI system before this divertor modification. Pumping speed from the three pumping ports is esti-

* Corresponding author. Tel.: +81 29 270 7343; fax: +81 29 270 7419; e-mail: itami@jt60rtm.naka.jaeri.go.jp

0022-3115/99/$ – see front matter
PII: S0022-3115(98)00855-1

mated to be 14 m^3/s for deuterium gas. There is no pumping slot at the outer divertor. Two gas puff positions were set for the divertor experiments. One was the main puff position which was located at the top of the vessel. The other was the divertor puff position, in which gas was injected through the pumping slot to the divertor region.

The bolometer arrays were used to measure radiation loss from the main and divertor plasmas and the VUV spectrometer was used to measure Ne X (1.21 nm) intensity in the main plasma. The 60 ch fiber optics with interference filters, of which chords was used to measure profiles of C II (657.8 nm), C IV (580.1 nm), D_a (656.1 nm) and Ne I (640.2 nm) in the divertor plasma.

The amount of neutral recycling in the divertor, $\Phi_{D_\alpha^{div}}$, and around the main plasma, $\Phi_{D_\alpha^{main}}$, are estimated from an integrating signal from an array of D_α diodes viewing the main and divertor plasmas, respectively. Details are described in Ref. [5].

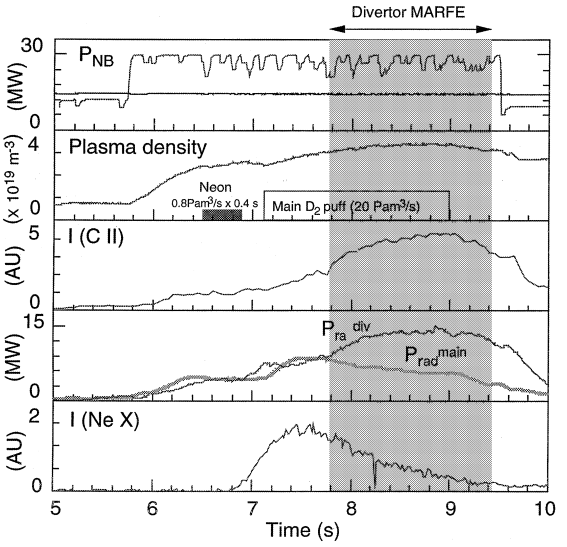

Fig. 1. Typical wave forms in this radiative divertor experiment. The neutral beam power of $P_{NB} = 25$ MW was applied to the target ELMy H-mode plasma with $I_p = 1.2$ MA and $B_T = 3.5$ T.

3. Neon exhaust and radiation profile change during the divertor MARFE

The radiative divertor experiment with the W-shaped divertor was carried out by applying a pulsed neon gas puff and intense D_2 puff to ELMy H-mode plasmas with $P_{NB} = 20$–25 MW, $I_p = 1.2$–1.5 MA and $B_T = 3.5$ T in JT-60U. Neon gas was injected in a pulse typically 0.8 Pa $m^3/s \times 0.4$ s) from the divertor puff position. Deuterium gas was injected continuously during NB heating phase from the main and divertor puff positions. We call the former 'the main D_2 puff' and the latter 'the divertor D_2 puff'. From the calculation of the conductance to the divertor and cryopumps, it is estimated that 30% of the divertor D_2 puff is pumped out without entering the divertor region.

Fig. 1 shows the typical wave forms in this experiment. The neutral beam power of $P_{NB} = 25$ MW was applied to the target ELMy H-mode plasma with $I_p = 1.2$ MA and $B_T = 3.5$ T. The plasma equilibrium in the divertor region was fixed in most of the discharges, as shown in Fig. 2(a). Radiation loss from the divertor, P_{rad}^{div}, increased after neon injection as Ne X intensity increased. However radiation loss from the main plasma, P_{rad}^{div}, was increasing after the main D_2 gas puff at $t = 7.1$ s. An additional boost of P_{rad}^{div} started at $t = 7.8$ s, the when the divertor MARFE started. Radiation loss from the divertor was gradually increasing up to $P_{rad}^{div} \sim 12$ MW at the end of the main D_2 puff. The divertor C II intensity has a similar wave form with P_{rad}^{div}. A decay of Ne X intensity indicates that the neon was pumped out from the main plasma at the time constant of 1.2 s. Radiation loss from the main plasma was also decreasing, while Ne X was decreasing. However, total radiation loss was unchanged after $t = 8.1$ s, the time when the divertor detachment was completed. In this paper, we refer the divertor detachment as the partial detachment in which the plasma detaches at both the inner and outer strike points of the separatrix. Decrease in the P_{rad}^{div} was compensated by increase in P_{rad}^{div} after $t = 8.1$ s. The divertor MARFE was sustained until the end of the main D_2 puff, while the radiation profile was gradually changing. During this period, the radiation loss from the edge plasma was decreasing and the radiation loss around the X-point was increasing.

Fig. 3 shows the relation between δP_{rad}^{div}, the incremental radiation after neon injection, the Ne X intensity for a discharge with only neon gas puffing (shot 29359) and a discharge with neon gas and main D_2 puffing (shot 29362). Here δP_{rad}^{div} is defined as

$$\delta P_{rad}^{div}(t) = P_{rad}^{div}(t) - P_{rad}^{div}(t_0),$$

where t_0 is the time when Ne X intensity started to increase. As is shown in Fig. 3, P_{rad}^{div} is coupled with Ne X intensity and enhanced by the main D_2 puff. Another important point in this figure is that P_{rad}^{div} decrease only by 35% in the later phase of the discharge without D_2 puff, since neon was hardly pumped out in the discharge.

4. Reduction of neutral back flow to the main plasma

It was demonstrated that neon puffing significantly reduced neutral back flow to the main plasma at the divertor detachment. In Fig. 4(a), the trajectory of P_{rad}^{total} is plotted against $\Phi_{D_\alpha^{main}}$, the main plasma recycling level, until the divertor detachment for shot 29362 and shot

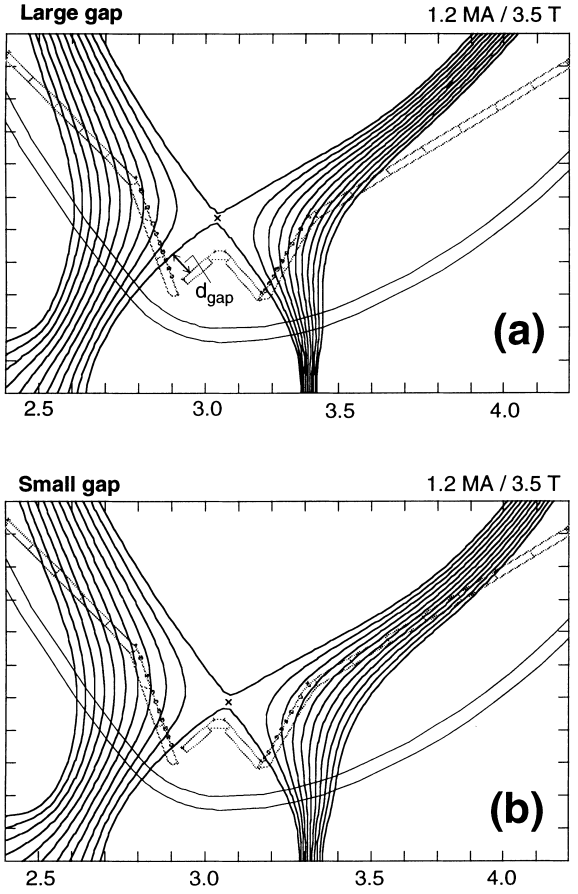

Fig. 2. The plasma equilibrium in the divertor with (a) the large gap and (b) the small gap.

31037. In shot 31037, only a main D_2 puff was applied. Total radiation loss from both the divertor and main plasma, P_{rad}^{total}, was almost same in the two discharges at the divertor detachment. In Fig. 4(b), trajectory of P_{rad}^{div} is plotted against $\Phi_{D_a^{inboard}}$, the divertor plasma recycling level at the inner divertor, for the same discharges. In the discharge with neon seeding,one half of the total radiation loss came from the main plasma when the divertor MARFE was triggered in shot 29362 and 7 MW of P_{rad}^{div} was enough as shown in Fig. 4(b). However, in the discharge without neon seeding, P_{rad}^{main} was as low as 3 MW and P_{rad}^{div} must be increased up to 10 MW for the divertor detachment. In order to obtain such a high radiation power from the divertor, 50 Pa m^3/s of main D_2 gas puff rate was needed at the time when the divertor MARFE started. This intense gas puff in shot 31037 resulted in larger $\Phi_{D_a^{inboard}}$ by a factor of five and larger neutral back flow, $\Phi_{D_a^{main}}$, by a factor of three than those in shot 29362. Since $\Phi_{D_a^{main}}$ was larger than the main D_2 gas puff rate by a factor of three, ionization of the neutral back flow from the divertor dominated the recycling level in the main plasma. In other words, neon injection reduced impacts on the main plasma by neutral back flow by a factor of three.

5. Peakedness of radiation power density near the X-point

It has been observed that radiation power concentrates near the X-point [3], when the divertor MARFE has established. From an engineering point of view, peakedness of radiation power density near the X-point must be controlled, since it is expected that the first wall facing the X-point will receive huge radiation power in a small surface area in fusion reactors. In ITER, for example, the heat load to the first wall must be lower than 5 MW/m^2. Therefore, uniformity in radiation loss in the divertor plasma must be improved. It was found that neon seeding was useful to suppress concentration of radiation power near the X-point during a divertor MARFE. In Fig. 5, peakedness of radiation loss is plotted against fraction of P_{rad}^{div} to P_{NB}. Peakedness of radiation power near the X-point is defined by the ratio of the radiation power density at ch 40 and ch 41 chords of the bolometer, i.e., P_{rad} (40 ch)/P_{rad} (41 ch). The ch 40 chord is 2.5 cm apart and the ch 41 chord is 6 cm apart from the X-point in the outer divertor, respectively. Data points in this figure were sampled every 50 ms from different type of discharges during the divertor MARFE phase in which P_{rad}^{total} exceed 70% of NB power. Strong peaking of the radiation loss was observed above $P_{rad}^{div}/P_{NB} = 0.7$. As shown in this figure, neon seeding provided a wide range of operations during the divertor MARFE phase. If P_{rad}^{div}/P_{NB} was controlled below this critical value over the whole period of the divertor MARFE, concentration of radiation power near the X-point was suppressed, as observed in shot 29362. In shot

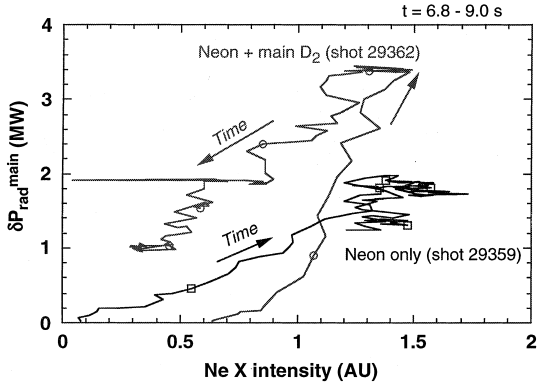

Fig. 3. Trajectory of the incremental radiation loss in the main plasma as a function of the Ne X intensity in the discharge with only neon gas puffing (shot 29359), and in the discharge with neon gas and the main D_2 puffing (shot 29362).

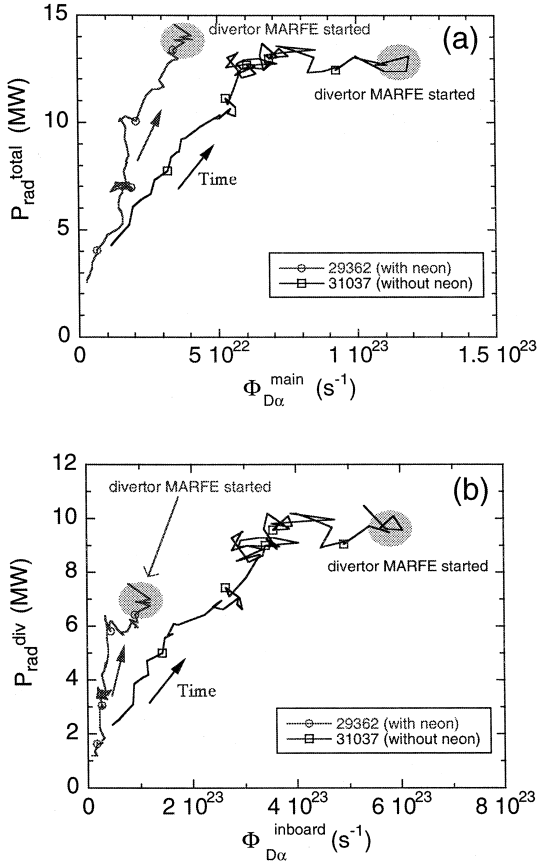

Fig. 4. (a) Trajectory of P_{rad}^{total} plotted against the main plasma recycling level for the discharge with (shot 29362) and without (shot 31037) neon seeding. (b) Trajectory of P_{rad}^{div} plotted against the divertor plasma recycling level at the inner divertor, for the same discharge with (a).

31015, P_{rad}^{main} was lower than that in shot 29362 and P_{rad}^{div} was larger than that in 29362 because of the different particle recycling and gas puff scenario. When P_{rad}^{div}/P_{NB} reached to 0.7 in a later phase of shot 31015, concentration of radiation power to the X-point was triggered and completed in about 150 ms, three samples in this figure. Without neon seeding (in shot 31037), operation range for less peaked radiation power density was very narrow. In those discharges, the peaking was often triggered by a sudden fault of one neutral beam which resulted in $P_{rad}^{div}/P_{NB} > 0.7$. The radiation power in the divertor could not decrease quickly enough to follow the sudden decrease of beam power.

6. Pumping efficiency of neon

Pumping efficiency of neon is characterized by exponential decay time of neon content in the main plasma. Here we represent the neon content by the Ne X

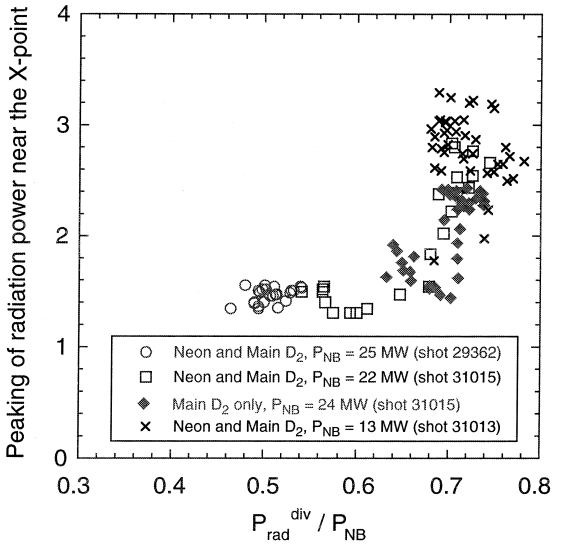

Fig. 5. Peakedness of radiation loss around the *X*-point during the divertor MARFE phase is plotted against P_{rad}^{div}/P_{NB} in the various discharges.

intensity measured by VUV spectroscopy. Both the main puff position and divertor puff position were used for D_2 puffing in order to study the effects on neon pumping. It was observed that neon decay time was effectively reduced by additional D_2 puffing. Decay time constant, τ_{neon}, was reduced to ~1 s in both the main and divertor D_2 puffs, while the required D_2 puff rate was different. For the main D_2 puff, 20 Pa m^3/s of gas puff rate was required and 40 Pa m^3/s for the divertor D_2 puff, as shown in Fig. 6. In the discharges with $I_p = 1.5$ MA and $B_T = 3.5$ T, τ_{neon} is shown as a function of

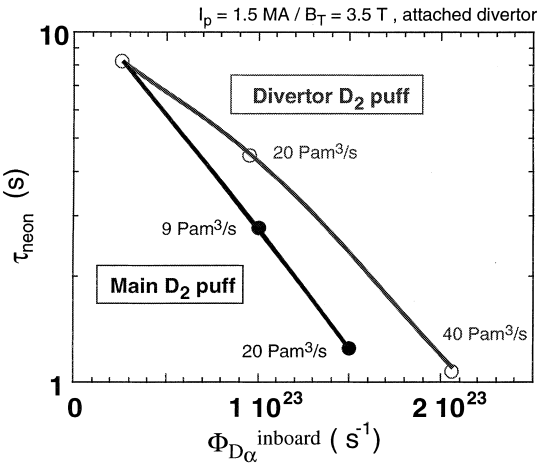

Fig. 6. τ_{neon} in the discharges with $I_p = 1.5$ MA and $B_T = 3.5$ T is shown as a function of $\Phi_{D_2^{inboard}}$, total particle flux to the inner divertor.

$\Phi_{D_a^{inboard}}$, total particle flux to the inner divertor. In this figure, τ_{neon} was calculated during the attached divertor phase. While it is estimated that 70% of the divertor D_2 puff is introduced to the main chamber, this figure shows that the main D_2 puff reduced neon decay time slightly better than the divertor D_2 puff.

7. Geometrical effect of the divertor configuration

In most of the discharges during this experiment, the separatrix at the inner divertor was fixed at the position where the slot-separatrix distance, d_{gap}, was 7.5 cm, as shown in Fig. 2(a). This divertor configuration might not be the optimum for impurity exhaust. Since 'escaping aperture' for neutrals increases as the inner separatrix approaches the pumping slot, the maximum pumping efficiency is expected at the minimum d_{gap} from geometrical considerations.

Neon and D_2 puffs were applied to the ELMy H-mode discharges in which $d_{gap} = 2$ cm and the other parameters are almost same. The divertor configuration in the discharges with the small gap is shown in Fig. 2(b). The prediction about tneon was confirmed when no additional D_2 puff was applied. The neon decay time τ_{neon} was 2.3 s in the discharge with the small gap, smaller by a factor of 3.5 than that in the discharges with the large gap. However, τ_{neon} with the small gap was not so much improved as the discharges with the large gap, when the main D_2 puff was applied. The neon decay time $\tau_{neon} = 1.6$ s at 1.5×10^{23} s^{-1} of $\Phi_{D_a^{inboard}}$ was even worse than τ_{neon} with the large gap.

We encountered difficulty in the discharges with the small gap in increasing the radiation loss from the main and divertor plasmas. The discharges with the small gap had lower P_{rad}^{div}/P_{NB} than that in discharges with the large gap. And δP_{rad}^{main}, as a function of Ne X intensity, was found to be smaller by a factor of three than the discharges with the large gap. Therefore, it was impossible to increase the total radiation power up to about 40% of the input power to trigger the divertor MARFE and divertor detachment, even if neon gas injection was increased up to fivefold and the main D_2 injection was doubled.

8. Discussions

It has already been investigated in the tokamaks with divertor pumping, such as ASDEX-U [6], DIII-D [7] and JET that pumping efficiency of neon was enhanced by additional D_2 gas puffing. This is the so-called puff and pump effect. The following three effects are expected to enhance the impurity exhaust. (1) Drag force to impurity ions toward the target by SOL flow, (2) high recycling effect and (3) ejection by ELM activity. However there is a controversy about the major contributor for the enhancement. DIII-D obtains the most effective impurity pumping when the divertor separatrix is close enough to the pumping opening and D_2 puff is applied from the top of the plasma. However ASDEX-U found that no significant difference by gas puff location and pointed out the pumping efficiency of neon increase with increasing divertor particle flux. The result in JT-60U shows the importance of the recycling level as is indicated by ASDEX-U. However, the effect of the gas puff location was also observed as in DIII-D.

The neon decay time τ_{neon} in the discharges with the large gap decreased significantly with increasing divertor recycling level, while τ_{neon} in the discharges with the small gap was improved only slightly. Fig. 7(a) shows time traces of Ne X intensity in the discharges with the large and small gap. In both the discharges, the same

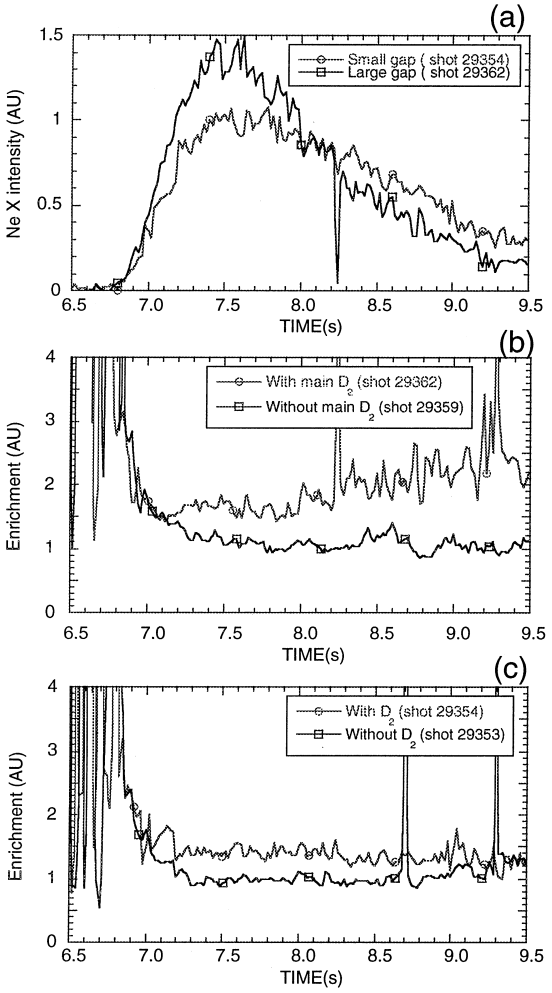

Fig. 7. Time traces of Ne X intensity in the discharges with the large and small gap. Time traces of divertor enrichment of neon in the discharges with (a) the large gap and (c) the small gap.

neon injection 0.8 Pa $m^3/s \times 0.4$ s from $t = 6.5$ s) and the same main D_2 puff rate of 20 Pa m^3/s were applied. In the discharge with the large gap, Ne X intensity increased rapidly and reached the maximum value larger than that with the small gap by 30%, probably due to poorer shielding to neon. However, neon was effectively pumped out in the later phase and Ne X intensity decreased to the level below that in the discharge with the small gap.

The ratio of I(Ne I)/I(Ne X) was used as the divertor enrichment of neon and was compared between discharges with the small gap and large gap. Here I(Ne I) was obtained by integrating Ne I profile over the divertor area. In Fig. 7(b) and (c), time traces of the divertor enrichment of neon are shown for the discharges with the large and small gap. When no D_2 gas puff was applied, both discharges have the same value of enrichment. However, the divertor enrichment of neon was significantly enhanced with the main D_2 puff in the discharge with the large gap. The enhancement was a factor of two in the later phase of the discharge in shot 29363. In the discharge with the small gap, the main D_2 puff enhanced the divertor enrichment of neon only by 30%. These results may be interpreted as follows. The first, geometrical effect dominated the neon exhaust when no gas puff was applied. The second, improvement of the divertor enrichment of neon by the main D_2 puff effectively reduced τ_{neon} even if the geometric aperture for neutral particles was poor.

9. Conclusions

For the purpose of controlling radiation profiles in the main and divertor plasmas, radiative divertor experiments were carried out with W-shaped pumped divertor of JT-60U. A pulsed neon gas puff and intense D_2 puff was applied to ELMy H-mode plasmas with $P_{NB} = 20$–25 MW, $I_P = 1.2$ to 1.5 MA and $B_T = 3.5$ T in JT-60U. D_2 gas puff enhanced pumping efficiency of neon content in the main plasma and reduced radiation loss from the main plasma. However the total radiation loss was unchanged and divertor detachment was sustained. Therefore the radiation profile control was successful during the divertor MARFE.

Peaking of radiation loss at the X-point was suppressed during the divertor MARFE, when P_{rad}^{div}/P_{NB} was below 0.7. Neon seeding and pumping enabled operation such that P_{rad}^{total} was larger than 70% of the input power without peaking of radiation power near the X-point.

Geometry to the pumping slot dominated the neon exhaust when no gas puff was applied. However, improvement of the neon enrichment caused by D_2 puff effectively reduced τ_{neon} even if the geometric aperture for neutral particles was small.

References

[1] K. Itami et al., Plasma Phys. controlled Fusion 36 (Suppl. 11A) (1995) A117.
[2] K. Itami et al., Fusion Energy Conference 1996, vol. 1, Montreal, International Atomic Energy Agency, Vienna, 1997, p. 385.
[3] N. Hosogane et al., J. Nucl. Mater. 220–222 (1995) 420.
[4] N. Hosogane et al., 1996 Fusion Energy Conference, Montreal, vol. 3, 1996, International Atomic Energy Agency, Vienna, 1997, p. 555.
[5] N. Asakura et al., these Proceedings.
[6] H.-S. Bosch et al., Phys. Rev. Lett. 76 (1996) 2499.
[7] M. Schaffer et al., J. Nucl. Mater. 241–243 (1997) 585.